Carbohydrate Research, 245 (1993) 43–56
Elsevier Science Publishers B.V., Amsterdam

Interaction of 8-anilino-1-naphthalenesulfonate with 2,6-di-*O*-methylcyclomaltoheptaose

Juziro Nishijo *, Mayumi Nagai and Masako Yasuda

Kobe Women's College of Pharmacy, Motoyama-kitamachi, Higashinada-ku, Kobe 658 (Japan)

(Received July 13th, 1992; accepted with revisions January 15th, 1993)

ABSTRACT

The interaction of 8-anilino-1-naphthalenesulfonate (ANS) with 2,6-di-*O*-methyl-cyclomaltoheptaose (2,6-DM-βCD) was investigated in a 0.1 M phosphate buffer at pH 7.4 by fluorescence spectrophotometry. Utilizing the fact that the fluorescence intensity of ANS increases in the presence of 2,6-DM-βCD, the thermodynamic parameters for inclusion complex formation were determined as follows: $\Delta G° = -10.3$ kJ·mol^{-1} at 25°C, $\Delta H° = -13.4$ kJ·mol^{-1}, $\Delta S° = -10.9$ J·deg^{-1}·mol^{-1}. The main driving force for the inclusion complex formation was considered to be the Van der Waals–London dispersion forces, while the contribution of the hydrophobic interaction was small. Also, from the measurements of proton nuclear magnetic resonance spectra and studies with Corey–Pauling–Koltun models, the probable structure was determined.

INTRODUCTION

8-Anilino-1-naphthalenesulfonate (ANS) is known to be a fluorescence probe for exploring hydrophobic regions in complex molecules[1]. The fluorescence of this agent is quenched in water, but in hydrophobic environments it is augmented substantially with shifts of the emission toward shorter wavelengths[2]. In addition, biological substances, such as proteins and biomembranes that have intramolecular hydrophobic regions, can interact with ANS to result in changes in the fluorescence spectra of ANS. Taking advantages of this property, ANS has been used to study the structure and functions of biological substances[3,4].

It has been reported that the fluorescence emitted by ANS increases when cyclomalto-oligosaccharides (cyclodextrins) such as cyclomaltooctaose (γCD) or cyclomaltoheptaose (βCD) are added to an aqueous solution[5,6]. The fluorescence intensity has been considered to originate from the presence of ANS in the hydrophobic cavity of the cyclodextrin molecule. Thus the hydrophobic bond is suggested as an important force in the formation of the inclusion complex between ANS and cyclodextrin. However, it was reported that the enthalpy term con-

* Corresponding author.

tributes more than the entropy term to the formation of the inclusion complex of βCD with ANS[7]. Further, we have reported similar results for the interactions of ANS with cyclomaltohexaose (αCD) and βCD[8,9].

In the present study, the authors investigated the interaction between ANS and 2,6-di-*O*-methyl-βCD (2,6-DM-βCD) by measuring the changes of fluorescence in the spectra of ANS in the presence of 2,6-DM-βCD in a phosphate buffer to clarify the effect of methylation on the interaction, 2,6-DM-βCD was selected because it has very high solubility in water and is expected to be the most useful host molecule for inclusion complexes[10]. The changes in enthalpy and entropy due to the formation of the inclusion complex were determined so that the driving forces acting between the components of the inclusion complex could be clarified. Further, the probable structure of the inclusion complex was determined by using Corey–Pauling–Koltun (CPK) models and by considering proton nuclear magnetic resonance (^{1}H NMR) data.

EXPERIMENTAL

Materials.—Reagent grade 2,6-DM-βCD, supplied by Nakarai Chemicals Ltd., was mainly mixtures of 2,6-DM-βCD and 2,6-di-*O*-methyl-mono(2,3,6-tri-*O*-methyl)-βCD when it was analysed by thin-layer chromatography on a Silica Gel 60-F_{254} HPTLC plate with 7:4:1 benzene–acetone–MeOH. Therefore, it was purified by semipreparative high-performance liquid chromatography on a Nova-Pak C_{18} cartrige (100 × 8 mm i.d.), eluting with 19:81 2-propanol–H_2O, and the material so purified was dried over P_2O_5 for 5 h at 110°C in a vacuum before use. Two forms of 8-anilino-1-naphthalenesulfonate (ANS) were also supplied by Nakarai Chemicals, Ltd. For ^{1}H NMR spectroscopy, the ammonium salt (twice recrystallized from water) was used, while the magnesium salt (also twice recrystallized from water) was used for the other experiments. The water was obtained by distilling water that had been twice purified with an ion-exchange resin.

^{1}H NMR.—^{1}H NMR experiments were all measured in deuterium oxide at 30°C. ^{1}H NMR experiments for determining the change of chemical shift were conducted on a Varian XL-200 (200 MHz) spectrometer with tetramethylsilane (Me_4Si) as an external reference. Aquisition time, 3 s; pulse angle, 90°; delay time, 2 s; number of transients, 96. Other ^{1}H NMR spectra were recorded on a Varian VXR-500 (499.8 MHz) spectrometer. Two-dimentional nuclear Overhauser enhancement spectroscopy (NOESY) experiments were performed using the State–Haberkorn method (2D hypercomplex method). A mixing time of 0.6 s and a relaxation delay, D_1, of 2 s were used. Two-dimensional rotating frame nuclear Overhauser effect spectroscopy (ROESY) experiments were performed in the phase-sensitive mode using the State–Haberkorn method. Spectra were acquired with 256 t_1 increments, and each increment consisted of 1 K data points from 16–32 transients. A spinlock mixing pulse of 250 ms was used.

Fluorescence spectra.—Fluorescence spectra were measured with a Shimadzu RF-503A recording fluorescence spectrometer in thermostatted cells at 5, 15, 25,

and 40°C. The change of temperature during the measurements was within 0.1°C. The lamp emission intensity changed only slightly during measurements, but in order to obtain reliable data, spectra were corrected by repeating the measurements of the standard sample after measurement of each sample.

Absorption spectra.—Absorption spectra were taken on a Shimadzu UV 300 spectrophotometer at 25°C. The measurements were carried out in 0.1 M sodium phosphate buffer, pH 7.4. The concentration of ANS was determined spectrophotometrically by taking the molecular absorptivity $\epsilon_{ANS} = 4950$ at 350 nm.

RESULTS AND DISCUSSION

Fig. 1 shows the effects of 2,6-DM-βCD on the absorption spectra of ANS. These spectra were measured, using a buffer solution containing the same concen-

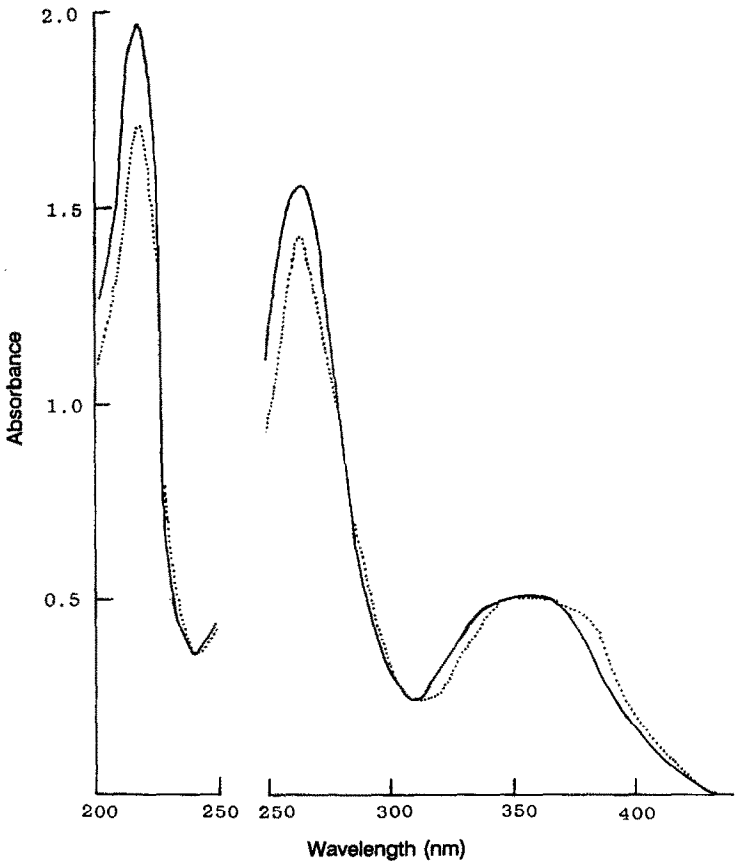

Fig. 1. Absorption spectra of ANS in the presence of 2,6-DM-βCD in 0.1 M sodium phosphate buffer, pH 7.4 at 25°C. In the region of 200–250 nm: ———, ANS only (4.9×10^{-5} M); ·····, ANS (4.9×10^{-5} M)+2,6-DM-βCD (2.0×10^{-2} M). In the region of 250–430 nm: ———, ANS only (1.0×10^{-4} M); ·····, ANS (1.0×10^{-4} M)+2,6-DM-βCD (1.0×10^{-2} M).

trations of 2,6-DM-βCD as the sample, as reference. The absorption spectra varied by adding 2,6-DM-βCD, although the changes were shown to be slight. The hypochromic effects at 218 and 266 nm, which are the absorption maximum wavelengths, were observed with only slight bathochromic shifts. Also, the absorption maximum at 353 nm, at which the isosbestic point was observed, increased. The changes of the absorption spectrum were closely similar to the case of βCD, though the changes were more marked than those observed for βCD.

Fig. 2 shows a part of the fluorescence spectra of 1.0×10^{-4} M of ANS measured in the presence of 2,6-DM-βCD at different concentrations in a 0.1 M phosphate buffer (pH 7.4) at 25°C. The concentrations of 2,6-DM-βCD ranged from 10 to 90 times higher than that of ANS. The fluorescence intensity increased as the concentration of 2,6-DM-βCD increased with a shift of fluorescence

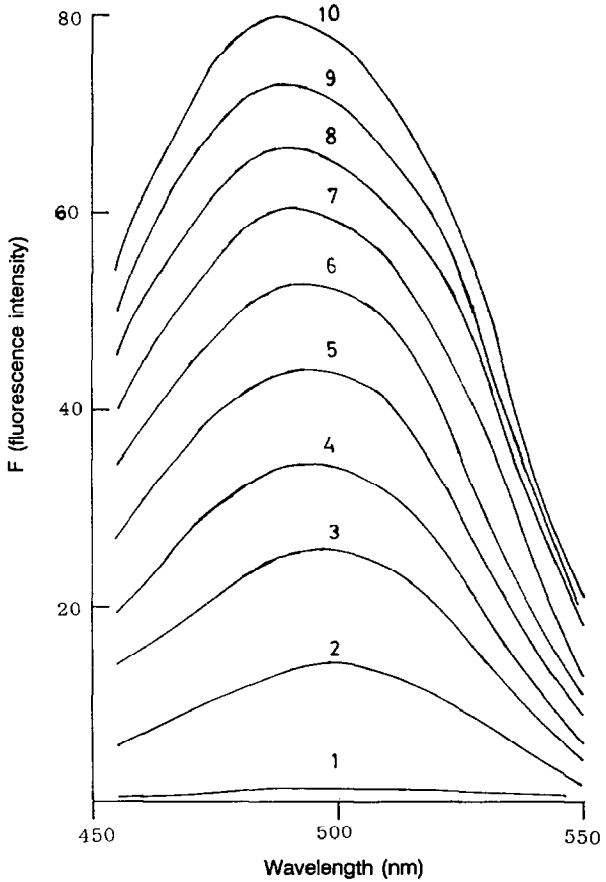

Fig. 2. Fluorescence spectra of ANS (1.0×10^{-4} M) in the presence of 2,6-DM-βCD in 0.1 M phosphate buffer, pH 7.4 at 25°C. 2,6-DM-βCD concentrations (M) are as follows: 1, 0; 2, 1.0×10^{-3}; 3, 2.0×10^{-3}; 4, 3.0×10^{-3}; 5, 4.0×10^{-3}; 6, 5.0×10^{-3}; 7, 6.0×10^{-3}; 8, 7.0×10^{-3}; 9, 8.0×10^{-3}; 10, 9.0×10^{-3}. The excitation wavelength was 365 nm.

maximizing at shorter wavelengths. These phenomena suggest that ANS molecules exist in an hydrophobic environment. Changes in the fluorescence and absorption spectra were not seen when either D-glucose or D-maltose was added in place of 2,6-DM-βCD; therefore, it is clear that interaction with 2,6-DM-βCD is closely related to the cavity of the cyclomalto-oligosaccharide.

As described above, the fluorescence intensity of ANS increases significantly in the presence of 2,6-DM-βCD. By taking advantage of this effect, the formation constant K was estimated. Assuming a 1:1 complex, when a large excess 2,6-DM-βCD is added to ANS, eq. (*2*) applies.

$$\text{DM-CD} + \text{ANS} \rightleftharpoons \text{DM-CD–ANS} \tag{1}$$

$$K = \frac{X}{C_0(A_0 - X)} \tag{2}$$

$$\Delta F = \Delta F_a + \Delta F_c \tag{3}$$

$$\Delta F = \frac{1}{1 + C_0 K}\Delta F_A - \frac{1}{1 + C_0 K}\Delta F_{\infty 1:1} + \Delta F_{\infty 1:1} \tag{4}$$

where C_0, A_0, and X represent total concentration of 2,6-DM-βCD, total concentration of ANS, and the concentration of ANS–2,6-DM-βCD complex, respectively. Also, DM-CD represents 2,6-DM-βCD. The fluorescence intensity (ΔF) observed is a sum of those of free ANS (ΔF_a) and complex (ΔF_c) (eq *3*). Eq (*4*) is valid where ΔF_A and $\Delta F_{\infty 1:1}$ denote the fluorescence intensity which should be observed when all ANS is free and all ANS has formed the ANS–2,6-DM-βCD complex, respectively. The formation constant K can be estimated from eq (*4*) using the nonlinear least-squares program, MULTI[12]. The values obtained at 5, 15, 25 and 40°C are shown in Table I. Also, Fig. 3 shows the binding curves for 2,6-DM-βCD with ANS, together with the theoretical curves obtained using the calculated parameters. The van't Hoff plots obtained by plotting log K against the absolute temperature are shown in Fig. 4. The changes in enthalpy (ΔH^0) and entropy (ΔS^0) accompanying the complexation were determined in the usual way. Each value obtained is given in Table I.

TABLE I

Thermodynamic parameters for Inclusion complex formation of ANS with 2,6-DM-βCD

(°C)	K [a] $(M^{-1})\times 10$	ΔG^0 $(kJ\cdot mol^{-1})$	ΔH^0 $(kJ\cdot mol^{-1})$	ΔS^0 $(J\cdot deg^{-1}\cdot mol^{-1})$
5	9.12	−10.0		
15	7.70	−10.0	−13.4 ± 1.3	−10.9 ± 1.3
25	6.32	−10.3		
40	4.79	−10.1		

[a] These values are averages, which were obtained form five repeat runs. Average probable errors are ±7% for K.

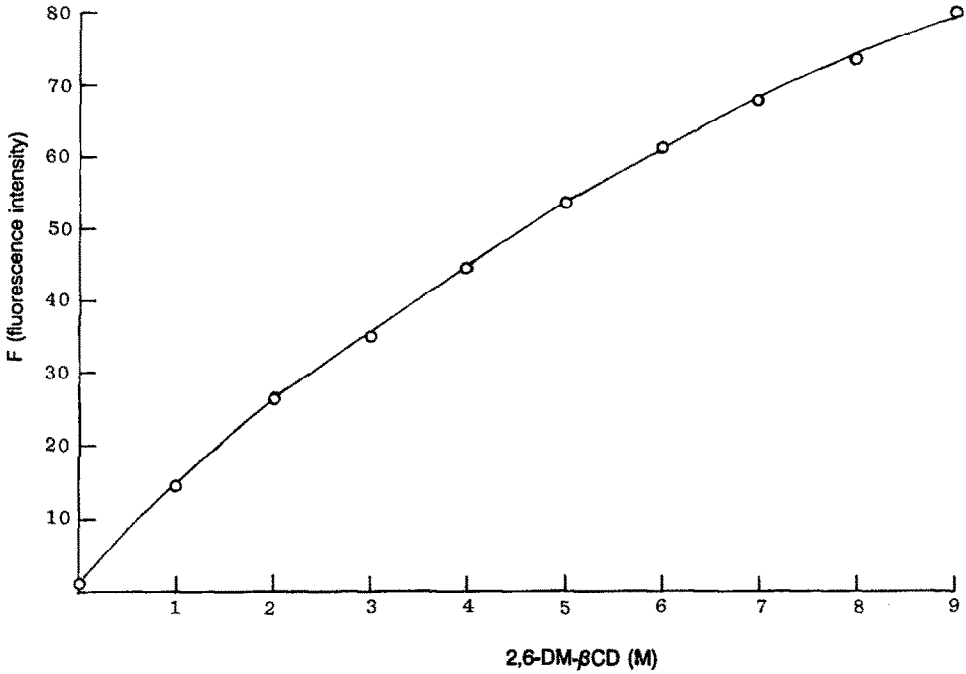

Fig. 3. Binding curve of 2,6-DM-βCD with ANS. ○, observed fluorescence intensity; ———, theoretical curve, which was obtained from eq (*4*) using the calculated parameters.

^{1}H NMR spectra and CPK models were used to estimate the structure of the inclusion complex between ANS and 2,6-DM-βCD. In Fig. 5(a), a ^{1}H NMR spectrum of 5.0×10^{-3} M ANS in deuterium oxide at 30°C is shown. The

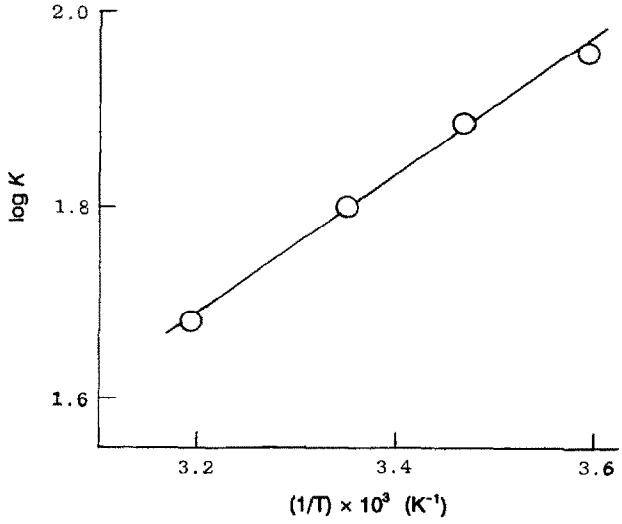

Fig. 4. The van't Hoff plot of the data in Table I.

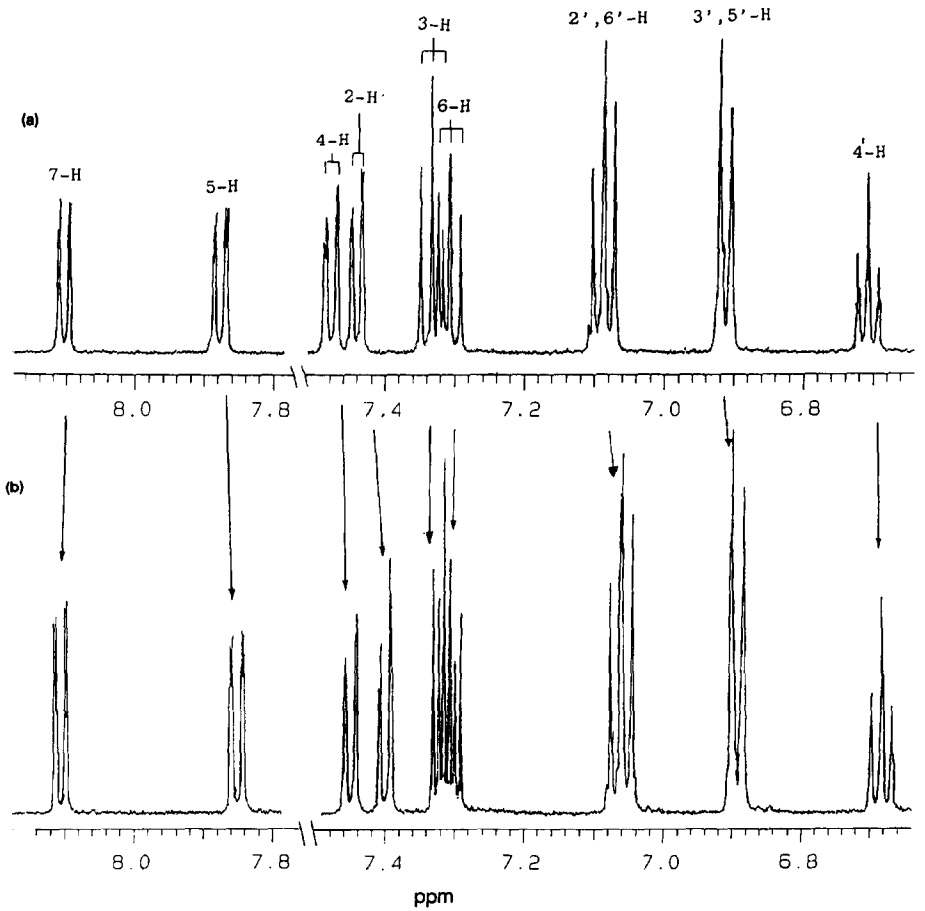

Fig. 5. ^{1}H NMR spectra of ANS in the presence of 2,6-DM-βCD in deuterium oxide at 30°C. (a) ANS alone (5.0×10^{-3} M); (b) ANS (5.0×10^{-3} M)+2,6-DM-βCD (5.0×10^{-3} M).

assignments of the proton signals of ANS have been reported[8]. The proton signals of ANS were shown to shift with the addition of 2,6-DM-βCD. In the presence of 5.0×10^{-3} M 2,6-DM-βCD, for example, as shown in Fig. 5(b), the proton signals of ANS shifted upfield, except for the signal due to H-7 of the naphthalene ring. The upfield shift of the H-2 signal was the most marked, and that of the H-6 signal was smallest. Also, the downfield shift of the H-7 signal was only slight. The order of the magnitudes of the upfield shifts of the signals due to the other protons were as follows; H-4 > H-5 $\geqq$ H-3',5' > H-4' > H-2',6' > H-3. The magnitudes of the shifts of the proton signals due to ANS in the presence of 2,6-DM-βCD at various concentrations are shown in Fig. 7(a).

A ^{1}H NMR spectrum of a 3.0×10^{-3} M solution of 2,6-DM-βCD is shown in Fig. 6(a). The assignments of the proton signals of the 2,6-DM-βCD were made on the basis of COSY measurements and values in the literature[13]. The spectrum varies in the presence of 5.0×10^{-3} M ANS as shown in Fig. 6(b). Comparison of

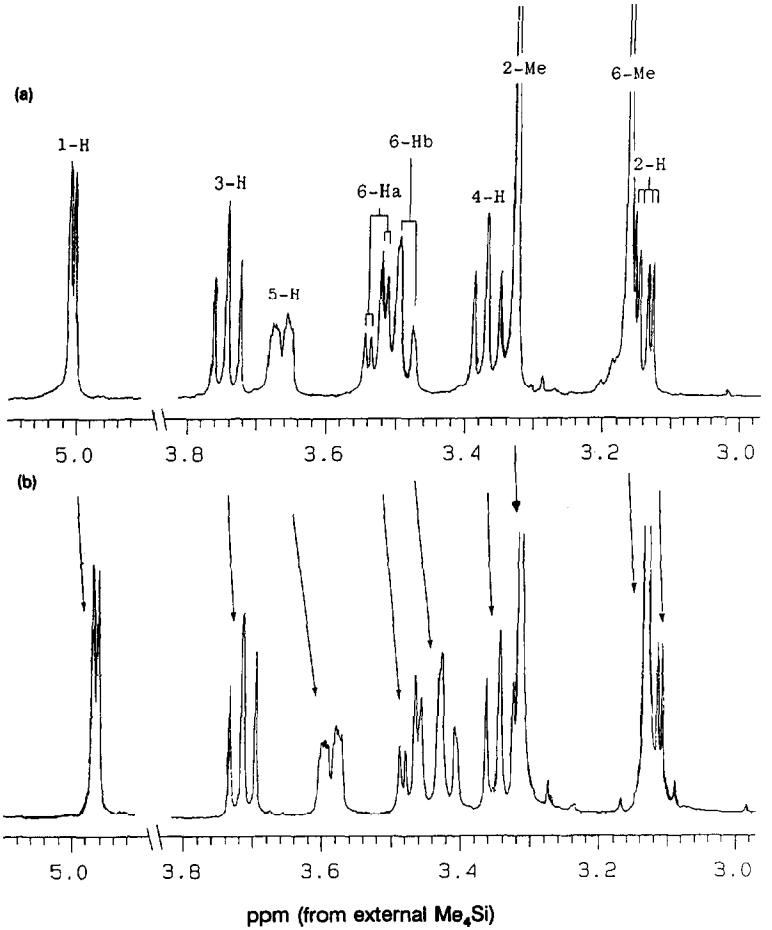

Fig. 6. ^{1}H NMR spectra of 2,6-DM-βCD in the presence of ANS in deuterium oxide at 30°C. (a) 2,6-DM-βCD alone (5.0×10^{-3} M); (b) 2,6-DM-βCD (5.0×10^{-3} M)+ANS (5.0×10^{-3} M).

these two spectra reveal that the signals due to protons of all types in the 2,6-DM-βCD molecule shifted upfield in the presence of ANS. The shift of H-5 was most prominent, followed by those due to H-6a and H-6b on the inner surface of the primary hydroxyl group side that was methylated. Also, the shifts of the signal due to H-1 on the outer surface of the cavity and one of the signals due to MeO-6 of the primary hydroxyl group that was methylated were most marked. On the other hand, the shifts of the signals due to protons on both surfaces of the secondary hydroxyl groups side were not so prominent. The magnitudes of the shifts of the proton signals due to 2,6-DM-βCD in the presence of ANS at various concentrations are shown in Fig. 7(b).

Three possible structures for the inclusion complex, judging from CPK models, are next considered (Fig. 8). These are described as follows: (*a*), all of the benzene ring and almost all of the naphthalene ring of ANS are enclosed in the cavity of

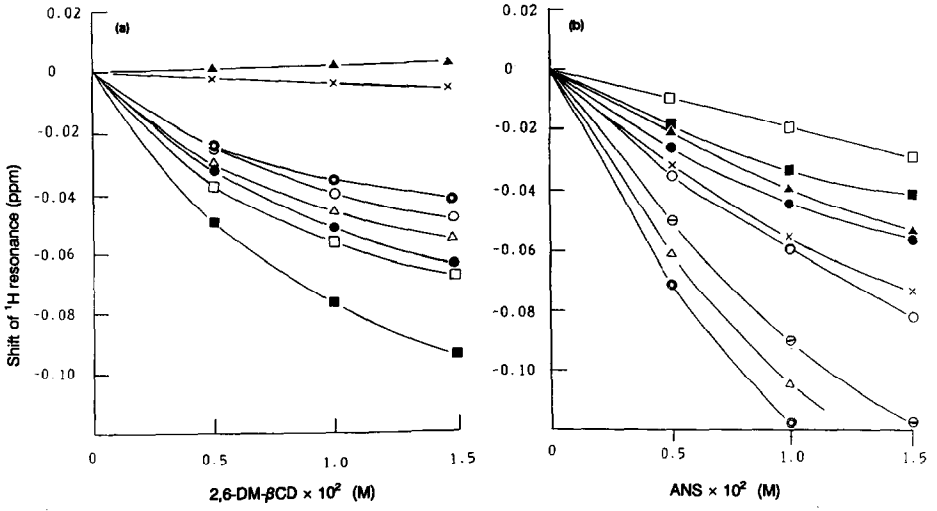

Fig. 7. (a) Induced ^{1}H NMR chemical shifts of ANS (5.0×10^{-3} M) in the presence of 2,6-DM-βCD. ■, H-2; □, H-4; ●, H-5, H-3′, H-5′; △, H-4′; ○, H-2′, H-6′; ⊙, H-3; ×, H-6; ▲, H-7. (b) Induced ^{1}H NMR chemical shifts of 2,6-DM-βCD (5.0×10^{-3} M) in the presence of ANS. ⊙, H-5; △, H-6b; ⊖, H-6; ○, H-1; ×, MeO-6; ●, H-3; ▲, H-4; ■, H-2; □, MeO-2. Signs + and − represent downfield and upfield shifts, respectively.

2,6-DM-βCD from the side of the secondary hydroxyl groups, which are positioned at the head of the benzene ring; (*b*), the benzene ring of ANS is enclosed in the cavity from the side of the primary hydroxyl group, with a larger part of the naphthalene ring remaining outside the cavity; (*c*), a large part of the naphthalene ring enters from the side of the secondary hydroxyl group, and the benzene ring is

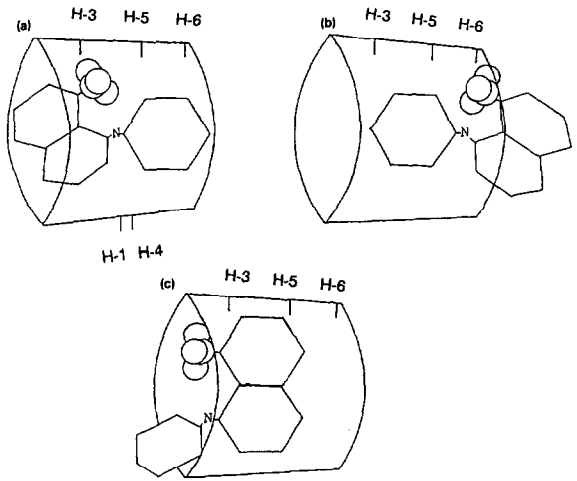

Fig. 8. Possible structures of the inclusion complex of ANS with 2,6-DM-βCD in aqueous solution based on CPK space-filling models.

almost outside the cavity. It is considered that the upfield shifts of the protons lying on the inner surface of 2,6-DM-βCD result mainly from the magnetic anisotropy of the benzene or naphthalene rings of the ANS molecule. The magnitudes of the upfield shifts of the proton signals are in the order H-5 > H-6a > H-6b > H-3. As the magnitudes of the upfield shifts of the H-6 signals due to 2,6-DM-βCD are greater than that of H-3, the structure in Fig. 8(c) does not seem plausible. From the structure in Fig. 8(b), the prominent upfield shifts of H-5 and H-3 signals can be rationalized, although the shift of H-5 would be expected to be greater than that of H-3. However, in Fig. 8(b) it would not be expected that the upfield shifts of the H-6 signals are greater than that of the H-3 signal, because the SO_3^- and =NH groups exist in the neighborhood of H-6, and the naphthalene and benzene rings do not have structural coplanarity, resulting in less deshieling for H-6 due to ring currents. Therefore, it was assumed that the inclusion complex cannot have the structure described in Fig. 8(b).

If the complex has the structure described in Fig. 8(a), it would not be surprising that the upfield shift of the H-5 signal is slightly larger than those of the H-6 signals, and that the shift of the latter is greater than that of the H-3 signal. Consequently, ANS is estimated to be enclosed in 2,6-DM-βCD in the manner illustrated in Fig. 8(a). To confirm the structure of the inclusion complex, a ROESY spectrum of the solution containing 2,6-DM-βCD (5.0×10^{-3} M) and ANS (5.0×10^{-3} M) in deuterium oxide was measured (Fig. 9). In the ROESY spectrum, the cross-peak connecting two proton resonances indicate that those proton nuclei are in close proximity in the ground state of the molecule. The unambiguous cross-peak was observed between the H-5 resonance of 2,6-DM-βCD and H-2′, H-6′ resonances of ANS. Also, the cross-peak is observed between the H-3 resonance of 2,6-DM-βCD and the H-6 resonance of ANS. Therefore, this supports the structure shown in Fig. 8(a).

DISCUSSION

Previously we reported the structure of the inclusion complex of ANS with βCD, as follows[8]: the entire benzene ring is enclosed in the cavity from the side of the primary hydroxyl groups of βCd to a considerable depth in the cavity, and a part of naphthalene ring is enveloped. This structure was derived from the measurements of the shifts of proton signals and from studies with CPK models. To confirm the structure of the inclusion complex of ANS with βCD, the ROESY spectrum of the solution containing ANS (2.0×10^{-2} M) and βCD (2.0×10^{-2} M) was measured. Cross-peaks connecting the H-5 resonance of βCD to the H-2′, H-6′, H-3′, and H-5′ resonances and the H-3 resonance of βCD to only the H-2′ and H-6′ resonances were observed. Therefore, it was found[14] that the probable structure of the complex between ANS and βCD is the one in which the entire benzene ring is enclosed in the cavity from the side of secondary hydroxyl groups of βCD to a considerable depth in the cavity, with a part of the naphthalene ring

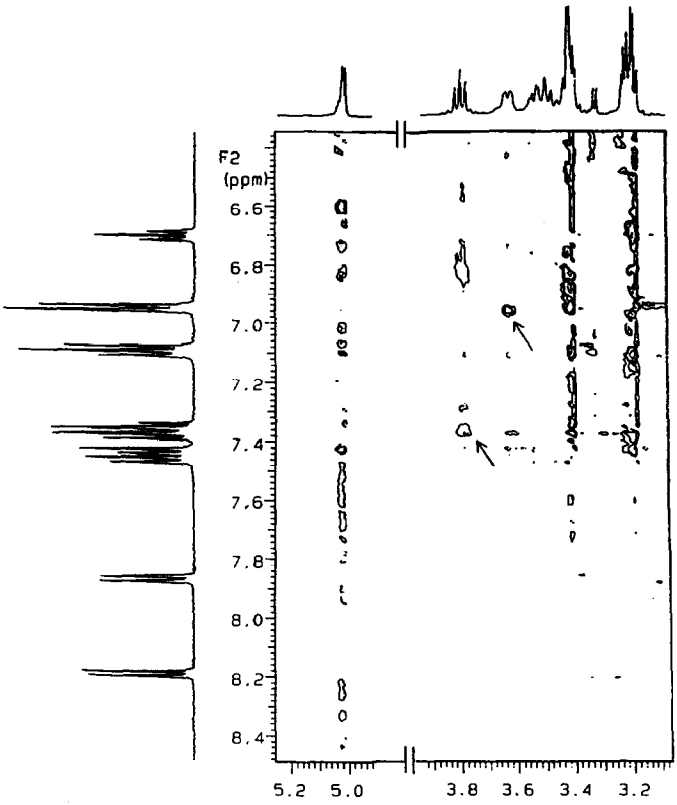

Fig. 9. 2D ROESY spectrum of the solution containing ANS (5.0×10^{-3} M) and 2,6-DM-βCD (5.0×10^{-3} M) in deuterium oxide. The most useful cross-peaks are indicated by arrows.

being enveloped. In the ROESY spectrum of the complex of ANS with 2,6-DM-βCD, the cross-peak connecting the H-3 resonance of 2,6-DM-βCD to the H-2′ and H-6′ resonances was not observed. This may occur because the cavity becomes deeper upon methylation, and consequently the benzene ring of ANS is more deeply enclosed in the cavity of 2,6-DM-βCD[15].

If the complex indeed has the structure shown in Fig. 8(a), the shifts of the signals due to included ANS can be explained as follows: The signals due to H-2, H-4, H-5, H-3′, H-5′, H-4′, H-2′, H-6′, H-3, and H-6 are shifted upfield as mentioned above. The upfield shifts of the proton signals due to the benzene ring might be caused by C–C bond anisotropy of 2,6-DM-βCD, and so on[16]. On the other hand, the protons of the naphthalene ring, except H-6 and H-7 do not exist at the position susceptible to C–C bond anisotropy, but reside in the neighborhood of the secondary hydroxyl groups. Therefore, the upfield shifts of the protons due to the naphthalene ring cannot be attributed to C–C bond anisotropy. Note that the upfield shift of the signal due to the H-2 of naphthalene adjacent to the SO_3^- group was most prominent. Consequently, it is considered that the prominent

upfield shift of the H-2 signal occurs because the SO_3^- group loses part of its hydrated water by entering the hydrophobic cavity from the aqueous solution, resulting in an increase in the electron density of H-2. Moreover, it is estimated that the electron densities at the positions of H-4, H-5, and H-7 increase more than those at the positions of H-3 and H-6 by the mesomeric effects due to SO_3^- group, and as the electron density increases, the proton signal shifts upfield. Also, it is considered that the benzene and naphthalene rings of ANS inside the complex are slightly more coplanar than in the deuterium oxide outside the cavity, because the signal due to H-2 and H-6 shift least upfield in the benzene protons, and the H-7 signals shift downfield only slightly, in spite of the increase in the electron density by the mesomeric effects mentioned above.

Now, the shifts of the proton signals due to 2,6-DM-βCD will be discussed for the structure shown in Fig. 8(a). It is reasonable that the upfield shift of the H-5 signal due to 2,6-DM-βCD is most prominent, followed by H-6a and H-6b, judging from the structure shown in Fig. 8(a). On the other hand, the upfield shifts of the signals due to protons, which exist on the side of secondary hydroxyl groups, are not as prominent as those due to the protons on the side of the methylated primary hydroxyl groups. This suggests that the coplanarity of aromatic rings does not increase so much upon the formation of an inclusion complex, because the plane of the naphthalene ring is aligned with the axis through the cavity of 2,6-DM-βCD. Also, the signals due to H-1, H-2, and H-4 lying on the outer surface of 2,6-DM-βCD are shifted upfield to different degrees. In spite of the fact that H-1 and H-4 lie on the outer surface and are almost the same distance from the entrance of the cavity, the upfield shift of the H-1 signal is larger than that of H-4. This may be due to conformational changes in the macrocycle upon complexation with ANS. It was assumed that conformational changes may have arisen from the torsion of the pyranose ring and may influence the position of H-1 more far than that of H-4, from the entrance of the secondary hydroxyl group side of the cavity.

In the case of complexation in an aqueous solution, van der Waals–London dispersion forces, hydrogen bonding, hydrophobic interactions, release of high-energy water molecules from the cavity of cyclodextrin, and the release of strain energy in a macromolecular ring of cyclodextrin, have all been reported to play a big part in the interaction[17]. However, according to Tabushi et al.[18], the van der Waals–London dispersion forces and hydrophobic interactions are major driving forces for inclusion complexation between cyclodextrin and a guest molecule. In the present study, it was found that the complexation is accompanied by negative changes in both enthalpy and entropy, suggesting that the van der Waals–London dispersion forces are mainly responsible for inclusion complex formation.

The thermodynamic parameters for complex formation of ANS with βCD were determined according to the procedure of Hana and Ashbaugh[8]. Assuming a 1:1 complex, reciprocals of the increases of the fluorescence intensities were plotted against fluorescence of βCD concentrations (which were present in excess). The thermodynamic parameters were determined as follows: $K = 70.9\ M^{-1}$ at 25°C,

$\Delta H^0 = -8.0$ kJ · mol^{-1}, $\Delta S^0 = 8.8$ J · deg · mol^{-1}. The two primary driving forces for complex formation of ANS with βCD were considered to be van der Waals–London dispersion forces and hydrophobic interactions. In the inclusion complex of ANS with βCD, the ANS moiety is rather loosely packed in the cavity. Therefore, it seemed reasonable that the change in enthalpy (ΔH^0) would be a small negative value, and the change in entropy (ΔS^0) would be a small positive one.

In the present study, as a possible structure of the inclusion complex between ANS and 2,6-DM-βCD, the structure shown in Fig. 8a was estimated. When the molecules are examined again using CPK models, it is clear that 2,6-DM-βCD has a wider entrance to the cavity than does βCD at the secondary hydroxyl group side, and it has a deeper cavity than βCD, resulting in ANS being enclosed more deeply and more tightly in the cavity of 2,6-DM-βCD than in the cavity of βCD. Therefore, the area of contact between ANS and 2,6-DM-βCD is greater than that of ANS and βCD, and the van der Waals–London dispersion forces acting between ANS and 2,6-DM-βCD are larger than those between ANS and βCD. This deeper penetration of ANS within the cavity of 2,6-DM-βCD produces not only a more favorable ΔH^0 due to the contribution of the van der Waals–London dispersion forces, but also a more unfavorable ΔS^0 due to the loss of the conformational freedom of 2,6-DM-βCD and/or the translational and rotational freedom of ANS. It is interesting that, on the whole, the formation constant, K, for the complex of ANS with 2,6-DM-βCD is slightly smaller than that for the complex of ANS with βCD over the temperature range investigated.

It has been reported[2] that there are two cases in which the fluorescence intensity increases. The first case, observed in a nonaqueous solvent, the coplanarity of the aromatic rings increased more than in aqueous solution. In the second case, conducted in a viscous solution, the motion of the ANS molecule was restricted more strongly than in an aqueous solution. In the present case, it is clear that the coplanarity of the aromatic rings of ANS increases more in the inclusion complex than in an uncomplexed form, as determined from the ^{1}H NMR spectra. Also, it is thought that the motion of the ANS molecule may be restricted more strongly in the inclusion complex than in the uncomplexed form. Therefore, the increase in fluorescence intensity can be attributed to both cases.

ACKNOWLEDGMENT

We thank Dr. M. Sugiura for her measurements of the ^{1}H NMR spectra.

REFERENCES

1 D.C. Turner and L. Brand, *Biochemistry*, 7 (1968) 3381–3390.
2 G.R. Penzer, *Eur. J. Biochem.*, 25 (1972) 218–228.
3 J. Romer and M.H. Bickel, *Biochem. Pharmacol.*, 28 (1979) 799–805.

4 H. Trauble and P. Overath, *Biochim. Biophys. Acta.*, 307 (1976) 491–512.
5 H. Kondo, H. Nakatani, and K. Hiromi, *J. Biochem. (Tokyo)*, 79 (1976) 393–405.
6 K. Miyazima, M. Sawada, T. Ueda, and M. Nakagaki, *Nippon Kagaku Kaishi*, 1984, 527–533.
7 G.C. Catena and F.V. Bright, *Anal. Chem.*, 61 (1989) 905–909.
8 J. Nishijo and M. Nagai, *J. Pharm. Sci.*, 80 (1991) 58–62.
9 J. Nishijo and M. Yasuda, and M. Nagai, *Chem. Pharm. Bull.*, 39 (1991) 5–9.
10 K. Uekama and T. Irie, *Seiyaku Kōjō*, 5 (1985) 20–23.
11 K. Koizumi, Y. Kubota, T. Utamura, and S. Horitama, *J. Chromatogr.*, 368 (1986) 329–337.
12 K. Yamaoka and T. Nakagawa, *J. Pharmacobio-Dyn.*, 6 (1983) 595–560.
13 M. Onda, Y. Yamamoto, Y. Inoue, and R. Chujo, *Bull. Chem. Soc. Jpn.*, 61 (1988) 4015–4021.
14 J. Nishijo, M. Yasuda, M. Nagai, and M. Sugiura, *Bull. Chem. Soc. Jpn.*, 65 (1992) 2869–2871.
15 K. Harata, *Bull. Chem. Soc. Jpn.*, 61 (1988) 1939–1944.
16 T. Nakajima, M. Sunagawa, T. Hirihashi, and K. Fujioka, *Chem. Pharm. Bull.*, 32 (1984) 383–400.
17 M. Komiyama and M.L. Bender, *J. Am. Chem. Soc.*, 100 (1978) 2259–2260.
18 I. Tabushi, Y. Kiyosuke, T. Sugimoto, and K. Yamamura, *J. Am. Chem. Soc.*, 100 (1978) 916–919.